Hindawi
Journal of Nanomaterials
Volume 2023, Article ID 6837264, 9 pages
https://doi.org/10.1155/2023/6837264

Research Article

Experimental Investigations on the Performance of Thermosyphon Solar Flat Plate Collector using TiO_2 Nanofluids

S. T. Jaya Suthahar,[1] S. Saravanan,[2] B. Karthikeyan,[3] S. Jaisankar,[4] R. Palanisamy,[5] Mohit Bajaj,[6,7] Mukesh Pushkarna,[8] and Sadam Alphonse[9]

[1]*Department of Mechanical Engineering, University College of Engineering, Thirukkuvalai, Nagapattinam 610204, India*
[2]*Department of Mechanical Engineering, K. Ramakrishnan College of Technology, Tiruchirappalli 621112, India*
[3]*Department of EEE, K. Ramakrishnan College of Technology, Tiruchirappalli 621112, India*
[4]*Department of Mechanical Engineering, Starlion College of Engineering and Technology, Thanjavur 614206, India*
[5]*Department of EEE, SRM Institute of Science and Technology, Kattankulathur, Chennai, India*
[6]*Department of Electrical Engineering, Graphic Era (Deemed to be University), Dehradun 248002, India*
[7]*Applied Science Research Center, Applied Science Private University, Amman 11931, Jordan*
[8]*Department of Electrical Engineering, GLA University, Mathura, India*
[9]*UFD PAI, Laboratory of Analysis of Simulation and Testing, University of Ngaoundere, P.O. Box 455, Ngaoundere, Cameroon*

Correspondence should be addressed to Sadam Alphonse; ssadamalphonse@yahoo.fr

Received 4 January 2023; Revised 2 February 2023; Accepted 8 February 2023; Published 22 February 2023

Academic Editor: Mohammad Rahimi-Gorji

Titanium dioxide nanofluid is used in the thermosyphon solar flat plate collector at volume fractions of 0.1%, 0.3%, 0.5%, 0.7%, and 1% to test the collector's effectiveness. The heat transfer coefficient, Nusselt number, friction factor, and pressure drop calculations were used to analyze the impact of adding nanoparticles to the working fluid. The effectiveness of the solar flat plate collector and the heat transfer coefficient are both greatly affected by the addition of titanium dioxide to the working fluid, with a tolerable rise in pressure drop. With concomitant variances of 15% and 13%, correlations were constructed for the Nusselt number and friction factor.

1. Introduction

Renewable energy is one of the most important sustainable energy resource for the future generation. The incident solar energy striking on the Earth's surface an hour is greater than all of the human consumption of energy in a year. Collecting and converting the solar thermal energy into something useful for the human needs is one of the most challenging tasks for researchers. Thermosyphon solar flat plate collector is one of the principle methods of collection of solar thermal energy, which vary drastically in the amount of solar flux captured as well as the method for capture. Heat transfer enhancement in a solar water heater is the process of improving the performance of a system. The most common type of solar flat plate collector utilizes a black surface as the absorber plate, which then transfers heat to a fluid running in the riser tubes embedded with the absorber plate surface. In this case, the efficiency is limited by how the absorber plate captures solar energy and also how effectively the heat is transferred to the working fluid. An approach that has been proposed to enhance the efficiency of solar collectors while improving the thermal performance of the system is using the nanofluid as a heat transfer medium. The conventional heat transfer fluids have a low thermal conductivity which limits their heat transfer rate. Suspension of nano-sized solid particles in the base fluid is an innovative way of enhancing the fluid's thermal performance. Nanofluid is a promising fluid for heat transfer enhancement due to its high thermal conductivity. Among the various passive techniques, nanofluids are used as a heat transfer medium in many engineering applications like heat exchangers, air heaters, and condensers also in solar collectors. Choi and Eastman [1] proposed nanofluid for heat transfer applications instead of conventional heat transfer fluids. Results show that nanofluids exhibit high thermal conductivities compare with conventional fluids for enhancement of heat transfer. Sekhar et al. [2] experimentally

investigated the thermal conductivities of water and Al_2O_3 nanofluid at low concentrations in the range of 0.05%–1%. Results indicate that enhancement of thermal conductivity increases with particle concentrations. Xuan and Li [3] investigated the convective heat transfer and flow features of nanofluids, effect of volume concentration, convective heat transfer coefficient, friction factor, and flow features. Albadr et al. [4] experimentally studied forced convective heat transfer and flow characteristics of nanofluid at different volume concentrations of Al_2O_3–water in heat exchanger, results indicate that increasing volume concentration increasing the viscosity and friction factor. Natarajan and Sathish [5] analyze the heat transfer properties of the nanofluids and compare the results with conventional fluids. The thermal conductivity of the carbon nanotubes/sodium dodecyl sulfate (CNT/SDS) dispersion has been investigated; thermal conductivity enhancement depends on the volume fraction of the suspended particle and thermal conductivity of the base fluids. And the experiment proves that the nanofluids more effective than conventional heat transfer fluids. Also, the possibility of using nanofluids in solar water heater for increasing the efficiency was clearly explained. Said et al. [6] used TiO_2 nanofluid and polyethylene glycol dispersant to evaluate the performance enhancement of solar flat plate collector in forced circulation mode. Energy efficiency, pressure drop, and pumping power were also calculated. Xuan and Roetzel [7] investigated the heat transfer mechanism of the nanofluid and proposing different methods to develop correlation for heat transfer. Khullar and Tyagi [8] studied the environmental impact of concentrating type solar water heater with nanofluid and a quantitative assessment for potential environmental benefits of solar water heater if substituted for those using fossil fuels. The proposed system introduces the experimental results of the material Al_2O_3–water-based nanofluid. Shareef et al. [9] experimentally studied the effect of Al_2O_3 nanofluid addition on the flat plate solar collector. The volume fraction of nanoparticles has been selected as 0.5%. The collector outlet, inlet temperatures difference increased with nanofluid than pure water for 1 l/min flow rates. Otanicar et al. [10] observed the improvement of 5% collector efficiency with nanofluid in the absorption medium with an increased efficiency with respect to increased volume fraction. Tyagi et al. [11] predicted efficiency of a direct absorption collector with nanofluid and found 10% higher efficiency compared to a flat-plate collector. Otanicar and Golden [12] reported the effective and economic utilization of nanofluids in the enhancement of solar collector efficiency. Yousefi et al. [13] investigated the effect of 0.2%, 0.4% with 15 nm Al_2O_3 nanofluid with and without surfactant and revealed the efficiency improvement of collector by 28.3% compared with water and surfactant. Said et al. [14] experimented natural and forced circulation on flat plate solar water heater with copper oxide nanofluid and observed addition of 0.05% volume fraction of nanopowder improved the thermal performance by 6.3%. Gangadevi et al. [15] studied the thermal efficiency of flat plate solar collector using Al_2O_3 nanofluid and observed an increase in volume fraction leads to an increase in the collector efficiency. In this work, the thermal performance of a flat plate solar collector employing MWCNT + Fe_3O_4/water hybrid nanofluids under thermosyphon conditions was examined. Various nanoparticle concentrations and Reynold's numbers were tested in the field. Theil's U2 was used to assess the prognostic paradigm's uncertainties which were found to vary from 0.0099 to 0.1544 for BOBRT [16–19].

From the literature, it is observed that most of the experimental studies were mainly focused on the use of nanofluids in forced circulation [20–22]. Hence, an experimental investigation to improve the thermal performance of solar collector was attempted using 0.1%, 0.3%, 0.5%, 0.7%, and 1% volume fractions of titanium dioxide nanopowder. Further, the Reynolds number, Nusselt number, heat transfer rate, friction factor, and thermal efficiency for the solar flat plate collector were calculated from the experimental facts and compared with water.

2. Materials and Methods

2.1. Experimental Setup. An experimental setup was fabricated to investigate the thermal performance and pressure drop behavior of TiO_2/water nanofluid in thermosyphon solar flat plate collector. The layout and photograph view of the experimental setup is shown in Figure 1 [23]. A riser tube was covered by black-coated absorbed plate. The cold fluid entered bottom side of riser tube and heated by black absorber plate and the hot fluid stored in top portion of tank. The unit has 2.2 m length and 0.22 m width and connected with insulated storage tank of 10 l capacity. This system working under natural buoyancy force is called thermosyphon effect. A transparent thin glass placed on the wooden cover and transmitted the solar energy to copper absorber plate and riser tube, and this setup called as leaf unit. The specification of the solar collector is given in Table 1. T-type thermocouples were brazed in absorber plate and riser tube, inlet and outlet temperatures of fluid were recorded by data logger. A magnetic flow meter was connected in the outlet of fluid passage which was used to measure the flow rate of the fluid.

2.2. Nanofluid Characterization. Nanofluid at different volume concentrations of 0.1%, 0.3%, 0.5%, 0.7%, and 1% is used to conduct the experiments. The TiO_2/water nanofluids are prepared from 99.7% pure nanodurable metal oxide powders supplied by Alfa Easer Ltd., USA, surface area of nanometal powder is 40 cm^2/g, and the density of the TiO_2 nanometal powder is 4,170 kg/m^3. Nanoparticle size plays a substantial role in enhancing the heat transfer of any thermal applications, increase in diameter of nanoparticle increases the viscosity of nanofluid and there is a great chance of increase in pressure in the riser tube. Hence, the TiO_2 nanopowder with the average particle size of 20 nm is used for nanofluid. Figure 2 shows the SEM (JSM-6390, JEOL Ltd., Peabody, Massachusetts) image of TiO_2 nanopowders; it reveals that the size of nanoparticle is in the range of 14.17–20.23 nm. Figure 3 shows the energy dispersive spectrum of TiO_2 nanoparticles, which reveals the 34.65 wt% of titanium and 64.35 wt% oxide. Through the one step method,

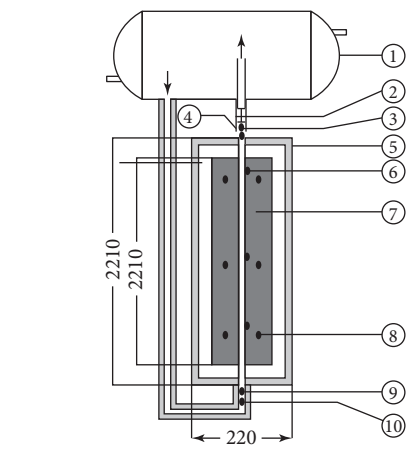

Figure 1: Layout and photographic view of the experimental setup.

Table 1: Specifications of solar flat plate collector.

S. no.	Design materials/parameters	Specifications
Collector		
1	Tilt angle	10° (South facing)
2	Aperture area, Ac	0.48 m^2
3	Collector glazing	Single transparent glass of 3 mm thickness
4	Riser tubes	OD 12.5 mm, ID 11 mm, length 2,000 mm
5	Absorber plate	Width 122 mm, length 2,000 mm
8	Bottom insulation	100 mm glass wool
9	Side insulation	60 mm glass wool covered by wooden frame
10	Absorber plate coating absorptivity	0.92
11	Transmittance of glazing	0.91
12	Number of riser tubes	1
Storage tank and piping		
13	Tank type	Vertical
14	Tank volume	10 l
15	Tank wall thickness	4 mm
16	Tank insulation thickness	50 mm
17	Connecting pipe size	ID 13 mm
18	Pipe insulation thickness	20 mm

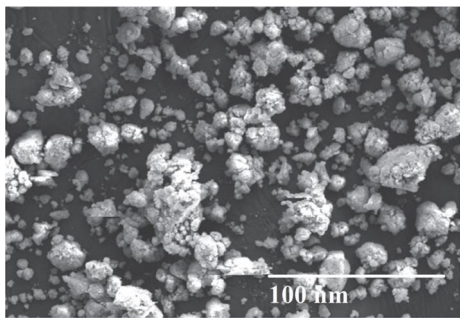

Figure 2: SEM image of the TiO_2 nanopowders.

nanofluid was prepared, with the required quantity of TiO_2 nanometal powder. With the help of magnetic stirrer, the fluid is enthused well and the sonication is done by using ultrasonic vibrating bath up to 1 hr. Stability of the nanofluid is measured for 0.1%, 0.3%, 0.5%, 0.7%, and 1% volume fractions. It is clear that the sonicated nanofluid has better stability and dispersion compared to unsonicated nanofluid. It is observed that the stability of TiO_2 nanoparticles for 0.1%, 0.3%, and 0.5% concentration is good (ζ/mV = −28) and almost it is stable for up to 14 days, whereas the stability of 0.7% and 1% volume concentrations is found to be moderate. The thermal conductivity of the nanofluid was measured

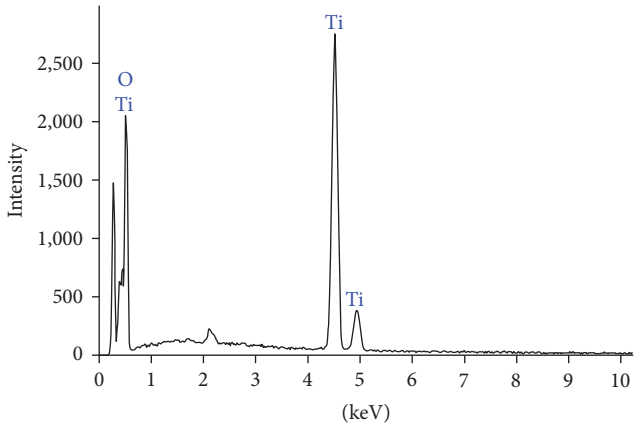

FIGURE 3: EDX image of the TiO_2 nanopowders.

with KD2 Pro thermal property analyzer, and values of the thermal conductivity are 19.1%, 24.3%, 28.7%, and 32.8% for 0.3%, 0.5%, 0.7%, and 1% volume concentrations, respectively.

2.3. Location of the Experimentation and Data Collection. The experimental work was carried out in Star Lion College of Engineering and Technology, Thanjavur, which is situated at 250 miles to the north of equator and its geographical location is 10°′N of latitude, 80°11′E of longitude and 88 m above mean sea level. The experimental work was performed during the period of March–June and the local weather conditions were measured. The day times are clear and bright sunny days, and 55% relative humidity present on those days with an average wind speed of 2.5 m/s and the average atmospheric temperature is 36°C. Six leaf units such as water, TiO_2/water nanofluid of volume concentration of 0.1%, 0.3%, 0.5%, 0.7%, and 1% are kept in open atmosphere with tilt angle of 10°. During the experimentation, data were recorded by data logger from 9.00 am to 4.00 pm at equal interval of every 15 min for 4 days and the readings are averaged and counted for calculations. Characteristics and heat transfer of thermosyphon solar flat plate collector have been divided into two phases, such as phase 1 (09:00–13:00 hours) and phase 2 (13:00–16:00 hours).

2.4. Data Processing. The correlations provided by Pak and Cho [24] and Equation (1) were used to calculate the density of the nanofluid:

$$\rho_{nf} = (1 - \varphi) + \varphi p_p. \tag{1}$$

The specific heat of the nanofluid is calculated by using Equation (2):

$$\left(\rho C_p\right)_{nf} = (1 - \varphi)\left(\varphi C_p\right)_f + \varphi\left(\rho C_p\right)_p. \tag{2}$$

Thermal conductivity of the nanofluid is calculated by using Equation (3) and it was introduced by Yu and Choi [25], as given below:

$$K_{nf} = K_f \frac{\left(K_p + 2K_f\right) - 2\varphi\left(K_f - K_p\right)}{\left(K_p + 2K_f\right) + \varphi\left(K_f + K_p\right)}. \tag{3}$$

The viscosity of the nanofluid is calculated by using Equation (4):

$$\mu_{nf} = (1 + 2.5\varphi)\mu_w. \tag{4}$$

The kinematic viscosity can be calculated by using Equation (5):

$$\nu = \frac{\mu}{\rho}. \tag{5}$$

Calculation of Reynolds and Prandtl numbers is as follows:

$$\Re = \frac{VD}{\nu}, \tag{6}$$

$$\Pr = \frac{\nu_{nf}}{\alpha_{nf}}. \tag{7}$$

Thermal diffusivity is given by the following equation:

$$\alpha_{nf} = \frac{k_{nf}}{\rho_{nf} C_p}. \tag{8}$$

The Nusselt number, thermal performance, and friction factor are calculated separately for phases 1 and 2.

The solar flat plate collector heat transfer rate is calculated based on the following equation:

$$Q = mC_p(T_{out} - T_{in}) = U_0 A_0 (T_{w0} - T_m). \tag{9}$$

The factors such as specific heat, mass flow rate, and inlet and outlet temperatures difference of fluid govern the heat transfer rate. By combining Equations (10) and (11), the internal convective heat transfer coefficient (h_i) is calculated and the values of the Nusselt number were obtained:

$$\frac{1}{(U_0 A_0)} = \frac{1}{(h_i A_i)} + \frac{\ln\left(\frac{D_0}{D_i}\right)}{(2\pi k_w L)}, \tag{10}$$

$$\mathrm{Nu} = \frac{h_i D}{k}. \tag{11}$$

Pressure drop measurement is done by using pressure transducers. The pressure drop is found to be more at low temperature and less at high temperature due to the decreased fluid viscosity with respect to the temperature rise. Based on the following equation, friction factor is calculated:

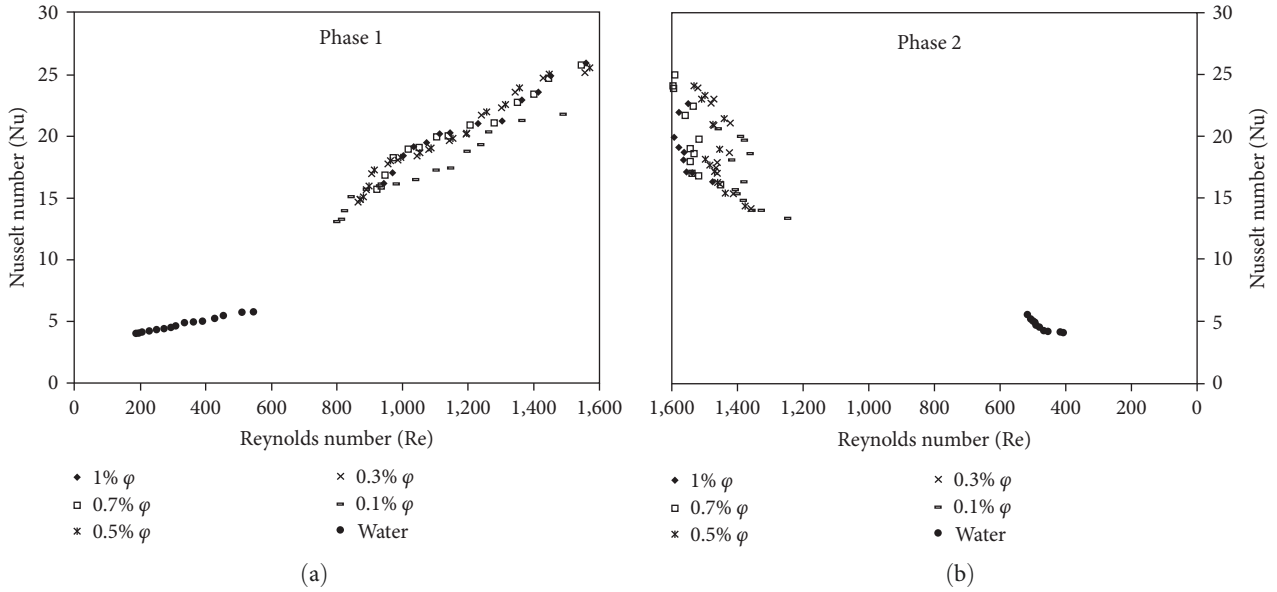

Figure 4: Nusselt number vs. Reynolds number in (a) phase 1 and (b) phase 2.

$$f = \frac{\Delta P}{\left(\frac{L}{D_i}\right)\left(\frac{\rho U_{m^2}}{2}\right)}. \quad (12)$$

With Hottel and Whillier equation, solar collector thermal performance is obtained:

$$\eta = F_R(\tau\alpha) - F_R U_L \frac{T_{in} - T_a}{H_t}. \quad (13)$$

Heat loss coefficient, heat removal factor, and transmittance–absorbance product are calculated by using Duffie and Beckman equation:

$$Q = H_t(\tau\alpha) - U_l(T_p - T_a), \quad (14)$$

$$U_l = \frac{Q - H_t(\tau\alpha)}{T_a - T_p}. \quad (15)$$

Based on Equation (17), heat removal factor is obtained:

$$Q = F_R(H_t(\tau\alpha) - U_l(T_{in} - T_a)), \quad (16)$$

$$F_R = \frac{Q}{H_t(\tau\alpha) - U_l(T_{in} - T_a)}. \quad (17)$$

Data reduction process is performed to find the experimental uncertainties with Coleman–Steele method and ASME. The maximum uncertainties are attained as ±1.9%, ±2.7, and ±3.3% for the Reynolds number, friction factor, and Nusselt number, respectively, with the thermal performance of ±1.17%.

3. Results and Discussion

3.1. Nusselt Number Data Verification. The theoretical values of Nusselt number for the plain water and the nanofluid at phases 1 and 2 are calculated and compared with experimental values with maximum deviation of ±7%. The values of the Reynolds number and Nusselt number gradually increase at phase 1 due to the high intensity of solar radiation which directly influences the mass flow rate and velocity of the working fluid, whereas the values of the Reynolds number and Nusselt number gradually decrease at phase 2 due to the reduction in the intensity of solar radiation.

Figures 4(a) and 4(b) show the Nusselt number vs. Reynolds number for phases 1 and 2. It is observed that the Nusselt number is found to be increased with respect to the increase in Reynolds number for all the conditions. When comparing with water, the Nusselt number is found to be higher for the TiO_2/water nanofluid with respect to the Reynolds number. The average values of the Nusselt number are obtained as 4.69, 16.29, 19.56, 19.97, 20.44, and 20.61 for plain water, 0.1% φ, 0.3% φ, 0.5% φ, 0.7% φ and 1% φ, respectively. It is perceived that the Reynolds number for the nanofluid of all conditions is found to be increased linearly with respect to the particle concentration and the Nusselt number for the nanofluid condition is found to be increased four times of the plain water. With the help of Gauss elimination method, a mathematical relationship was developed for phases 1 and 2 conditions with 95% of confidence level and their values were compared with the experimental values.

3.2. Enhancement of Heat Transfer in Nanofluids Collectors. The values of heat transfer coefficient with respect to Reynolds number of a thermosyphon solar flat plate collector with nanofluid are presented in Figures 5(a) and 5(b) that show the convective heat transfer coefficient with respect to

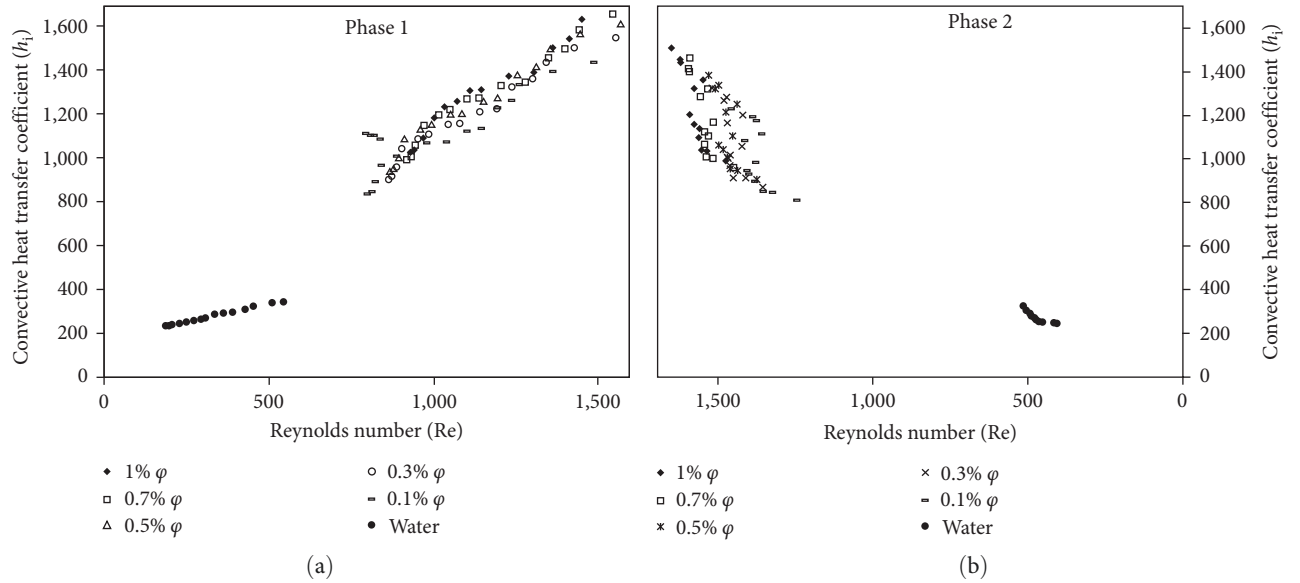

Figure 5: Convective heat transfer coefficient vs. Reynolds number (a) phase 1 and (b) phase 2.

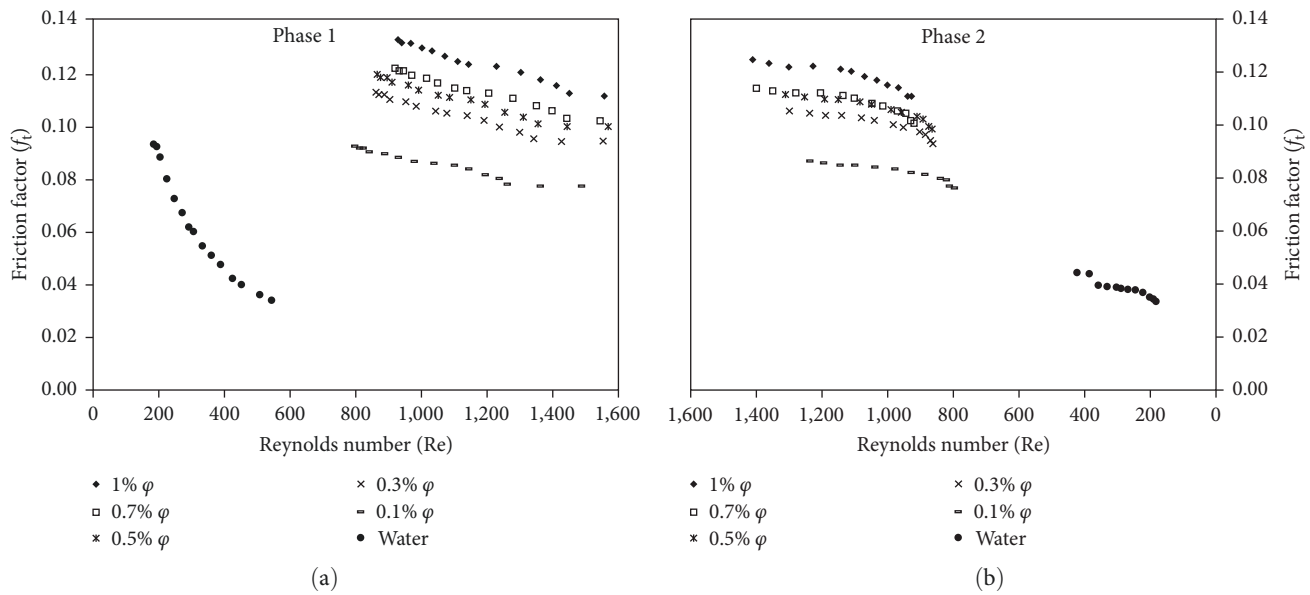

Figure 6: Friction factor vs. Reynolds number (a) phase 1 and (b) phase 2.

the Reynolds number for water, titanium dioxide–water nanofluid at varying volume concentrations of 0.1%, 0.3%, 0.5%, 0.7%, and 1%. The heat transfer for the TiO_2 nanofluid is found to be higher when compared to plain water. Thermal conductivity of the fluid is enhanced by the addition of titanium oxide nanoparticles in the base fluid, which results in the increase in heat transfer by compared to the plain water collector. The average value of h_i for both phases 1 and 2 were obtained as 754.89, 787.44, 829.42, 877.05, and 904.17 W/m^2K for 0.1%, 0.3%, 0.5%, 0.7%, and 1% volume concentrations, respectively, which indicates the intensification of increase in heat transfer coefficient directly proportional to the particle volume concentration. Though the viscosity of the nanofluid increases with an increase in particle volume concentration which leads to decrease in heat transfer rate and Nusselt number, whereas the minimum percentage reduction of Nusselt number is observed at lower particle concentrations.

3.3. Friction Factor and Pressure Drop. The suspended TiO_2 nanoparticle increases the density of the base fluids and it leads to increase in viscosity and friction factor. Figures 6(a) and 6(b) show the variation in the friction factor with respect to the Reynolds number. The friction factor is found to be increased by 9%, 13%, 21%, 31%, and 37% for 0.1% φ, 0.3% φ, 0.5% φ, 0.7% φ, and 1% φ, respectively, which indicates that

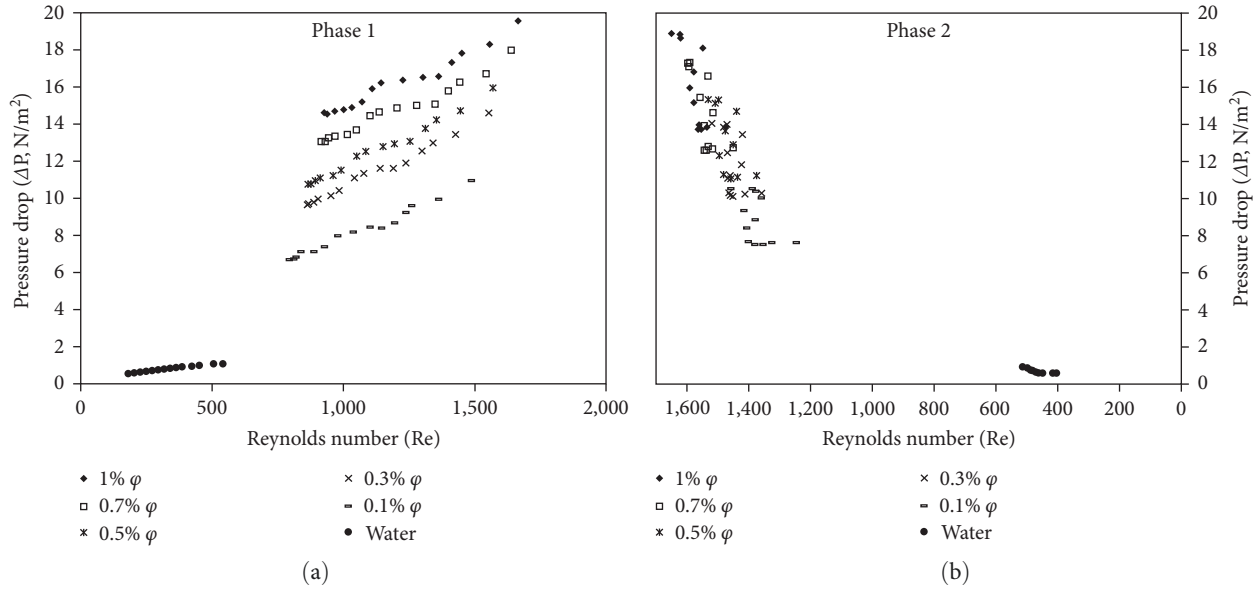

Figure 7: Pressure drop vs. Reynolds number (a) phase 1 and (b) phase 2.

the friction factor increases linearly with the volume concentration of nanoparticle in base fluid. Friction factor is a function of Reynolds number and particle volume fraction. The predicted values of friction factor were compared with the experimental values. Figures 7(a) and 7(b) show the variation in the pressure drop with respect to the Reynolds number. It is observed that pressure drop increases with the increase in friction factor due to nanoparticle concentration in the base fluid. The pressure drop is found to be higher for the higher concentration of nanoparticles, i.e., 1% volume concentrations whereas the pressure drop is found to be much lower for the water. From the pressure drop measurements, the average percentage increase for the 0.1% φ, 0.3% φ, 0.5% φ, 0.7% φ, and 1% φ TiO_2 nanofluid is in the order of 90.51%, 92.81%, 93.78%, 94.60%, and 95.21% of the pressure drop due to the occurrence of nanoparticles in the working fluid when compared with water.

3.4. Thermal Performance. Several factors influence the collector's instantaneous efficiencies such as absorber plate design, type of coating, coating material, glazing property, and the condition of operation. Figure 8 shows the efficiency curve for the flat plate solar collector at different volume concentrations of TiO_2 nanofluid. It is found that there is an increase in the instantaneous efficiency with an increase in solar radiation insolation. During phase 1, the instantaneous efficiency of the system is increased due to the increase in heat transfer whereas the instantaneous efficiency of the system is decreased in phase 2. The efficiency of TiO_2 nanofluid collector is found maximum when compared with the water collector because of the fact that the surface area of the fluid increases with increase in nanosized metal particle suspended in working fluid which influences the heat removal rate from the absorber plate to working fluid, whereas in case of the water, the surface area is less compared with nanofluid that results in the reduced heat removal rate. It is found that

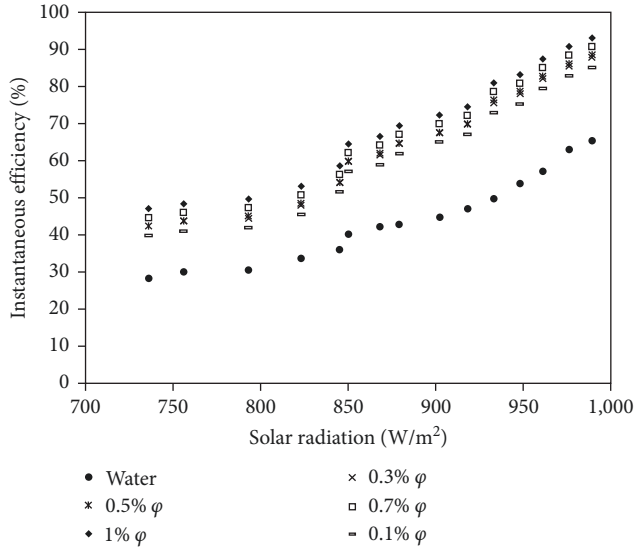

Figure 8: Instantaneous efficiency of solar flat plate collector.

collector with nanofluid of 0.1% φ, 0.3% φ, and 0.5% φ is rectilinear under the specified operating conditions. In collector with plain water minimum amount of heat is removed from the absorber plate and the rate of heat removal is 0.61. In case of TiO_2 nanofluid, the heat removal factor gradually increases with increase in particle volume concentrations. The average heat removal rate for phases 1 and 2 for 0.1% φ, 0.3% φ, 0.5% φ, 0.7% φ, and 1% φ are found as 0.88, 0.91, 0.93, 0.96, and 0.98, respectively. This indicates that the fluid thermal conductivity has a relatively strong influence on the mean plate temperature and heat removal rate solar flat plate collector. Thermal efficiency of the collectors with 0.3% φ and 0.5% φ was increased by almost 31% and 42%, respectively, when compared with the water tube

collector, which shows the TiO_2 nanofluid gives a significant increment in efficiency with insignificant drop in the pressure. The temperature of the absorber plate is the quantification of heat transfer between the riser tube and working fluid and it is found to be increased with an intensity rise of the solar radiation and atmospheric temperature during phase 1. The heat removal rate is found to be higher for the nanofluid collector from the absorber plate when compared with the water collector.

4. Conclusion

The effectiveness of the titanium dioxide nanofluid at concentrations of 0.1%, 0.3%, 0.5%, 0.7%, and 1% in plain water and the thermosyphon solar flat plate collector was tested. It was discovered that when the volume concentration of TiO_2 grew, the heat transfer coefficient increased and the pressure drop dropped; the resulting values were 77.21% and 16.08 N/m^2, respectively. In comparison to water, the TiO_2 nanofluid's immediate thermal efficiency is found to rise with increasing volume concentration; a greater instantaneous thermal efficiency of 91% is recorded at 1% TiO_2 nanofluid.

Nomenclature

A_c: Collector aperture area, m^2
A_i: Inside surface area of the riser tube, m^2
A_o: Outside surface area of the riser tube, m^2
C_p: Specific heat, kJ/kg°C
D_o: Outside riser tube diameter, m
f: Friction factor for water tube collector, (dimensionless)
f_{nf}: Friction factor for nanofluids collector, (dimensionless)
H_t: Total intensity of solar radiation, W/m^2°C
k: Thermal conductivity of water, W/m°C
k_w: Thermal conductivity of the riser tube wall, W/m°C
L: Length of the riser tube, m
m: Mass flow rate, kg/s
Nu: Nusselt number for water riser tube, dimensionless
Nu_{nf}: Nusselt number for nanofluid
Pr: Prandtl number, dimensionless
Q: Heat transfer rate, W
Re: Reynolds number based on the internal diameter of the riser tube, dimensionless
d_p: Diameter of the nanoparticle, nm
S: Surface area of the particle
C_{pnf}: Heat capacity of the nanofluid
C_{pf}: Heat capacity of the base fluid
C_{pp}: Heat capacity of the nanoparticles
T_m: Bulk mean temperature of fluid in the riser tube, °C
T_{in}: Average outlet temperature of water, °C
T_{out}: Average outlet temperature of water, °C
T_{wo}: Average wall surface temperature outside
U_i: Overall inside heat transfer coefficient, W/m^2K
U_o: Overall outside heat transfer coefficient, W/m^2K
U_l: Overall heat loss coefficient, W/m^2K
η: Collector efficiency
F_R: Collector heat removal factor
$\tau\alpha$: Transmittance–absorptance produce
U_l: Overall heat loss coefficient
T_a: Ambient temperature
T_p: Absorber plate temperature
H_t: Total solar radiation

Greeks

ρ: Density of water, kg/m^3
φ: Volume fraction of nanoparticle, %
μ: Dynamic viscosities of water at bulk mean temperature, Ns/m^2
μ_w: Dynamic viscosity at wall temperature, Ns/m^2
ΔP: Pressure drop of water, N/m^2.

Data Availability

Data available on request.

Conflicts of Interest

The authors declare that they have no conflicts of interest.

References

[1] S. U. S. Choi and J. A. Eastman, "Enhancing thermal conductivity of fluids with nanoparticles," in *1995 International Mechanical Engineering Congress and Exhibition*, pp. 99–105, ASME, 1995.

[2] Y. R. Sekhar, K. V. Sharma, M. T. Naik, and L. S. Sundar, "Experimental investigations on thermal conductivity of water and Al_2O_3 nanofluids at low concentrations," *International Journal of Nanoparticles*, vol. 5, no. 4, pp. 300–315, 2012.

[3] Y. Xuan and Q. Li, "Investigation on convective heat transfer and flow features of nanofluids," *ASME Journal of Heat and Mass Transfer*, vol. 125, no. 1, pp. 151–155, 2003.

[4] J. Albadr, S. Tayal, and M. Alasadi, "Heat transfer through heat exchanger using Al_2O_3 nanofluid at different concentrations," *Case Studies in Thermal Engineering*, vol. 1, no. 1, pp. 38–44, 2013.

[5] E. Natarajan and R. Sathish, "Role of nanofluids in solar water heater," *The International Journal of Advanced Manufacturing Technology*, 2009.

[6] Z. Said, M. A. Sabiha, R. Saidur et al., "Performance enhancement of a flat plate solar collector using titanium dioxide nanofluid and polyethylene glycol dispersant," *Journal of Cleaner Production*, vol. 92, pp. 343–353, 2015.

[7] Y. Xuan and W. Roetzel, "Conceptions for heat transfer correlation of nanofluids," *International Journal of Heat and Mass Transfer*, vol. 43, no. 19, pp. 3701–3707, 2000.

[8] V. Khullar and H. Tyagi, "A study on environmental impact of nanofluid-based concentrating solar water heating system," *International Journal of Environmental Studies*, vol. 69, no. 2, pp. 220–232, 2012.

[9] A. S. Shareef, M. H. Abbod, and S. Q. Kadhim, "Experimental investigation on a flat plate solar collector using Al_2O_3 nanofluid as a heat transfer agent," *International Journal of Energy and Environment*, vol. 6, no. 4, pp. 317–330, 2015.

[10] T. P. Otanicar, P. E. Phelan, R. S. Prasher, G. Rosengarten, and R. A. Taylor, "Nanofluid-based direct absorption solar collector," *Journal of Renewable and Sustainable Energy*, vol. 2, no. 3, Article ID 033102, 2010.

[11] H. Tyagi, P. Phelan, and R. Prasher, "Predicted efficiency of a low-temperature nanofluid-based direct absorption solar

collector," *Journal of Solar Energy Engineering*, vol. 131, no. 4, pp. 410041–410047, 2009.

[12] T. P. Otanicar and J. S. Golden, "Comparative environmental and economic analysis of conventional and nanofluid solar hot water technologies," *Environmental Science & Technology*, vol. 43, no. 15, pp. 6082–6087, 2009.

[13] T. Yousefi, F. Veysi, E. Shojaeizadeh, and S. Zinadini, "An experimental investigation on the effect of Al_2O_3–H_2O nanofluid on the efficiency of flat-plate solar collectors," *Renewable Energy*, vol. 39, no. 1, pp. 293–298, 2012.

[14] Z. Said, P. Sharma, L. S. Sundar et al., "Improving the thermal efficiency of a solar flat plate collector using MWCNT-Fe_3O_4/water hybrid nanofluids and ensemble machine learning," *Case Studies in Thermal Engineering*, vol. 40, Article ID 102448, 2022.

[15] R. Gangadevi, S. Senthil Raja, and I. Syed Adil, "Efficiency analysis of flat plate solar collector using Al_2O_3 nanofluid," *Indian Streams Research Journal*, vol. 2, pp. 1–4, 2013.

[16] Z. Said, P. Sharma, L. Syam Sundar, V. G. Nguyen, V. D. Tran, and V. V. Le, "Using bayesian optimization and ensemble boosted regression trees for optimizing thermal performance of solar flat plate collector under thermosyphon condition employing MWCNT-Fe_3O_4/water hybrid nanofluids," *Sustainable Energy Technologies and Assessments*, vol. 53, Part C, Article ID 102708, 2022.

[17] S. Ping and S. A. A. Shah, "Green finance, renewable energy, financial development, FDI, and CO_2 nexus under the impact of higher education," *Environmental Science and Pollution Research*, 2022.

[18] R. Manikandan, S. Sekar, S. Pugal Mani, S. Lee, D. Y. Kim, and S. Saravanan, "Bismuth tungstate-anchored PEDOT:PSS materials for high performance HER electrocatalyst," *International Journal of Hydrogen Energy*, 2023.

[19] A. Munusamy, D. Barik, P. Sharma, B. J. Medhi, and B. J. Bora, "Performance analysis of parabolic type solar water heater by using copper-dimpled tube with aluminum coating," *Environmental Science and Pollution Research*, 2023.

[20] A. Ghozatloo, A. Rashidi, and M. Shariaty-Niassar, "Convective heat transfer enhancement of graphene nanofluids in shell and tube heat exchanger," *Experimental Thermal and Fluid Science*, vol. 53, pp. 136–141, 2014.

[21] Y. Wang, H. A. I. Al-Saaidi, M. Kong, and J. L. Alvarado, "Thermophysical performance of graphene based aqueous nanofluids," *International Journal of Heat and Mass Transfer*, vol. 119, pp. 408–417, 2018.

[22] Z. Said, P. Sharma, R. M. Elavarasan, A. K. Tiwari, and M. K. Rathod, "Exploring the specific heat capacity of water-based hybrid nanofluids for solar energy applications: a comparative evaluation of modern ensemble machine learning techniques," *Journal of Energy Storage*, vol. 54, Article ID 105230, 2022.

[23] S. T. J. Suthahar, S. Jaisankar, and S. Saravanan, "Experimental investigation on solar flat plate collector using alumina nanofluid with tube inserts," *Materials Technology*, vol. 37, no. 3, pp. 179–189, 2022.

[24] B. C. Pak and Y. I. Cho, "Hydrodynamic and heat transfer study of dispersed fluids with submicron metallic oxide particle," *Experimental Heat Transfer*, vol. 11, no. 2, pp. 151–170, 1998.

[25] W. Yu and S. U. S. Choi, "The role of interfacial in the enhancement thermal conductivity of nanofluid: a renovated Maxwell model," *Journal of Nanoparticle Researchs*, vol. 5, pp. 161–171, 2003.